SEISMIC PERFORMANCE OF LARGE RC CIRCULAR HOLLOW COLUMNS

Giulio RANZO[1] And M J N PRIESTLEY[2]

SUMMARY

experimental study conducted on three large size specimens are reported. The test units, designed with only one layer of longitudinal and spiral reinforcement near the outside face, were subjected to constant compressive axial force and cyclically varying lateral load. Theoretical aspects of the shear strength degradation with increasing lateral displacement are approached with recently developed shear strength models and with the Modified Compression Field Theory. Predictions of the behavior and of the failure mode are compared with the experimental results, showing good agreement.

The first unit failed in flexure in a ductile fashion, while the second and the third failed in shear in a ductile and brittle fasion respectively. In all tested units concrete spalled off in the inside face, causing rapid strength degradation. Results indicate that a ductile performance is obtained with relatively low levels of longitudinal reinforcement and axial load. The shear strength enhancement due to the effect of the axial load appears to be less significant than in solid member

INTRODUCTION

performance of structural components to be used for the construction of new bridges. As a part of this on-going research task, the University of California San Diego has completed an experimental program on the shear strength and ductility capacity of thin wall circular hollow columns. The program was sponsored by the California Department of Transportation (Caltrans).

Previous research in this field has shown that this type of structural member may be, in some cases, economically viable when compared to usual solid members. Applications include large bridge columns and piles as well as offshore platforms. This structural type was in fact extensively used in Europe and in Japan since the early seventies. The economical convenience in the use of hollow columns is due to the cost saving afforded by reduced section area (up to 70%). Also, hollow columns are more efficient than solid ones from a structural point of view. When the weight of the vertical members is relevant in the performance of the entire structure, a significant reduction in the seismic mass may be attained by using this structural type.

Zahn et al. [Zahn et al.,1990] and Whittaker et al. [Whittaker et al.,1987] investigated the ductility capacity of slender circular members without confinement on inside face. It was found that a ductile behavior is obtained with low amounts of longitudinal reinforcement, low levels of axial load and reasonably thick wall. In Japan, the Tokyu Construction Company has instead conducted a study on the behavior of slender and squat circular members with two layers of reinforcement and crossties [Tokyu Cnstr. Co.,1998]. These units, designed in accordance with the requirements of the Japanese railways, had a rather thick wall (about 20% of the section diameter) and performed in an extremely ductile manner. Unfortunately, in this latter case the cost reduction due to the use of smaller amounts of concrete is conterbalanced by high construction costs required to place two layers of reinforcement and crossties.

This paper presents the results of an investigation on the aspects that still remained unknown : in particular, the shear strength of simple systems with only one layer of reinforcement near the outside face. The results confirm the findings obtained for more slender members, indicating that the implosion of concrete in the inside surface governs the activation of the strength degradation mechanism. Considerations are made on the methods to be used to predict the maximum strength and deformation capacity of members characterized by a small ratio of the

[1]   PhD Student, University of Rome "La Sapienza", Rome, Italy – Email : granzo@dsg.uniroma1.it
[2]   Professor of Earthquake Engineering, University of California San Diego, La Jolla, CA, USA

shear span to the section diameter. State-of-the-art shear strength models [Priestley et al.,1998] are used, with some modifications, and results are compared with more sophisticated sectional analysis conducted with the Modified Compression Field Theory [Bentz and Collins, 1998][Collins and Vecchio, 1986]. In both cases, comparison with experimental evidence shows good agreement in terms of ultimate strength and deformation capacity as well as load-deformation behavio

DESIGN AND ANALYSIS

the section diameter **D**. In solid members, the restraint provided by the transverse steel against concrete dilatancy generates a confining action in terms of an inward radial pressure. In contrast, in thin-wall circular hollow members the action of transverse steel generates circumferential compression stresses on the tubular wall. In this case, the radial component of the confining stress is rather low and does not contribute to the enhancement of the concrete strength. However, circumferential stresses may be rather high (particularly in case of very thin wall), providing a considerable increase in concrete peak strength and deformation. This desirable mechanism becomes less effective if the concrete spalls off near the inside surface under the effect of high bending and shear forces.

Design for flexure has therefore to account for the effect of this particular type of confinement on the concrete performance. The confining pressure can be estimated based on equilibrium considerations, as suggested in [Paulay and Priestley,1992] for solid sections. A modification is suggested to account for the hollow shape of the section, by considering that the total force applied by the transverse reinforcement is acting on a curved thin wall rather than on a solid core. Thus, it is proposed the effective pressure f_l be estimated as :

$$f_l = \frac{2 f_{sh} A_h}{D' s A_r} \tag{1}$$

where f_{sh} is the stress in the transverse reinforcement, A_h is the area of transverse steel, **D'** is the diameter of the part of the section enclosed by transverse steel, s is the spacing of the transverse reinforcement and A_r is the ratio of the section net area to the section gross area. Based on the value of f_l , the confined concrete properties can be computed (according to the Mander model) by using the equations suggested in [Paulay and Priestley,1992]. For this purpose, a reduction coefficient of 0.7 is suggested for the confining pressure f_l , for conservative design.

As discussed above, when these members are subjected to flexure and high compressive strains occur, concrete tends to spall off near the inside surface, since no restraint is provided against inward implosion. Experience showed that ultimate flexural capacity is generally reached when the compressive strain near the inside face reaches 0.006-0.008. The flexural behavior (up to failure) can be estimated with usual techniques based on moment-curvature analysis.

Usual condiderations are made in regard to the problem of longitudinal rebar buckling. The spacing of transverse steel should be less than 6 bar diameters, as suggested in [Paulay and Priestley,1992] in order to avoid buckling between two adjacent layers of hoop reinforcement.

Design for shear can be made by using the shear strength model "UCSD-D", with the design equations suggested by Priestley et al [Priestley et al.,1998]. The nominal shear capacity is expressed as the sum of three independent components :

$$V_N = V_c + V_s + V_p \tag{2}$$

where :

$$V_c = \alpha\beta\gamma\sqrt{f_c'}\,(0.8 A_{sn}) \tag{3}$$

$$V_s = \frac{\pi}{2} A_h f_{yh} \frac{D - c - co}{s} \cot\theta \tag{4}$$

$$V_p = 0.85 P \frac{D - c}{2L} \tag{5}$$

In equation (3) A_{sn} is the section shear area, while α, β and γ are factors for aspect ratio, longitudinal reinforcement and ductility respectively, where :

$$1 \le \alpha = 3 - M/VD \le 1.5 \tag{6}$$

$$\beta = 0.5 + 20\left(\frac{A_{st}}{A_n}\right) \le 1 \quad \text{if} \ \ c \ge t \quad \text{or} \quad \beta = 0.5 + 20 \frac{A_{st}}{\pi D^2/4} \quad \text{if} \ \ c < t \tag{7}$$

$$A_{sn} = \frac{(1 + \lambda^2)(1 - \lambda)}{(1 - \lambda^3)} A_n \tag{8}$$

$$\begin{array}{ll} \gamma = 0.25 & \mu_\phi \leq 3 \\ \gamma = 0.25 - 0.0167(\mu_\phi - 3) & 3 \leq \mu_\phi \leq 15 \\ \gamma = 0.05 & \mu_\phi \geq 15 \end{array} \tag{9}$$

In eqn. (4) c is the depth of the compression zone at nominal flexural capacity, co is the concrete cover to main longitudinal rebars, f_{yh} is the yield stress of transverse steel and $\theta=35°$ is the angle of inclination of the diagonal cracks. In eqn. (5) P is the axial load and L is the length of inflection. In eqn. (7) A_{st} is the area of the longitudinal steel. In eqn. (8) $\lambda=D_i/D$, where D_i is the inside diameter of the section. Eqn. (8) expresses the shear area of a hollow circular section as a function of the wall thickness, where A_n is the net area of the concrete section. Eqn. (9) describes the mechanism according to which the concrete contribution to shear strength V_c decreases with increasing curvature ductility μ_ϕ.

From the original version of the model [Priestley et al.,1998], modifications were made (in eqns. (7) and (8)) to account for the effective shear area (the λ coefficient) and the position of neutral axis with respect to the inside column face (option on the value of the β factor). The effect of the axial load component V_p on hollow members is not yet completely understood. In fact, it appears that the beneficial effect of a compressive axial force on shear strength is less effective in hollow columns than in similar solid members. The arching action has to develop along a curved thin wall rather than on a solid portion of concrete resulting in a radial component of force which induces hoop tension. For conservative design, the axial load contribution to shear strength (as expressed by the V_p component) should probably be neglected.

The prediction of the force-displacement behavior can be made based on sectional analysis of the column base region. The flexural behavior of the column base section can be estimated with moment-curvature analysis. The shear behavior instead can be determined based on the available shear strength as a function of the curvature ductility. For this purpose the UCSD shear model should be used in the assessment case (UCSD-A). This implies that a coefficient of 100/85 has to be applied to the γ factor and to the V_p component and that an angle $\theta=30°$ has to be assumed in eqn (4). These modifications essentially take off the conservative margins adopted in the design equations, in oder to obtain the best estimate of shear capacity.

The flexural displacement at the column top can be computed with the concept of equivalent plastic hinge length [Paulay and Priestley,1992], while the shear displacement can be computed based on the predicted strain in the transverse reinforcement [Priestley et al.,1996]. In the case of a member subjected to single bending, the top displacement is found as :

$$\Delta = \frac{\phi_y' L^2}{3} + \left(L - \frac{L_p}{2}\right)(\phi - \phi_y') + \varepsilon_t L \tag{10}$$

where the first term is the elastic flexural displacement component, the second term is the plastic flexural displacement component and the third is the shear displacement component. In eqn(10), ϕ_y' is the curvature at first yield of longitudinal rebars, L_p is the plastic hinge length, ε_t is the strain in the transverse reinforcement and L is the length of inflection. The values of ε_t are found from the actual values of the V_s component, according to the procedure described in [Priestley et al.,1996]. Along the force-displacement curve, the actual value of V_s is found as :

$$V_s = V - (V_c + V_p) \tag{11}$$

From the actual value of V_s the actual value of the stress in the transverse reinforcement f_s can be found from a generalized form of eqn. (4),where f_{yh} is replaced by f_s and the equation is solved for f_s.Once the stress f_s is known, the corresponding strain can be found by assuming a bilinear constitutive behavior for the transverse steel. The plastic hinge length is estimated with the following expression :

$$L_p = 0.08L + 0.022 f_y d_{bl} \tag{12}$$

where f_y is the yield stress of longitudinal bars in MPa, while d_{bl} is the bar diameter in mm.

The force-displacement behavior can also be predicted with a pushover analysis, using the MCFT [Bentz and Collins,1998]. This model incorporates the effects of combined flexure and shear under the general assumptions of the engineering beam theory [Collins and Vecchio,1986

SPECIMENS, TEST SETUP AND INSTRUMENTATION

Following the considerations presented in the previous section, three specimens were designed. The same geometry and amount of transverse reinforcement was used for all units, while different levels of longitudinal reinforcement and axial load were considered. The main characteristics of the tested specimens are summarized in the following Table 1:

Table 1 – Properties of the test units

Specimen	M/VD	D (mm)	t (mm)	$P/f_c'A_n$ (%)	Long. rebars (mm)	Trans. Reinf. (mm)	f_c' (MPa)
HS1	2.5	1560	152	0.05	68 D13	D6 @ 70	40
HS2	2.5	1524	139	0.05	68 D16	D6 @ 70	40
HS3	2.5	1524	139	0.15	68 D16	D6 @ 70	35

For all units, nominal properties of longitudinal and transverse steel are indicated in the following Table 2:

cover : 13mm (to main long. rebars)
Long. reinf. : 34 bundles of 2 bars

1244mm 1524mm
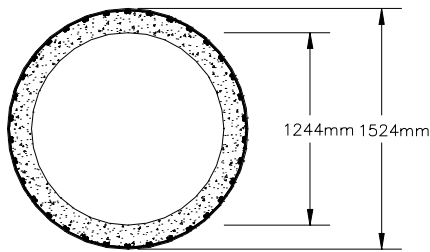
Figure 1 – Section geometry and

Table 2 – Steel mechanical properties

Type	E_s (Gpa)	f_y (MPa)	f_u (MPa)	ε_u
Long. Rebars	195	450	700	0.08
Spiral	165	635	820	0.015

The transverse reinforcement consisted of a continuous spiral. The longitudinal reinforcement ratios, referred to the concrete net area are 0.014 for unit HS1 and 0.023 for units HS2 and HS3. The volumetric ratio of transverse reinforcement (referred to the net concrete volume) is 0.0035. The section geometry with the arrangement of longitudinal and transverse reinforcement is shown in fig.1.

The first unit (HS1), characterized by low levels of longitudinal reinforcement and axial load was designed to fail in flexure. The second (HS2), characterized by a higher level of longitudinal reinforcement was instead designed to fail in shear. The third (HS3), with the same longitudinal reinforcement as HS2 and a higher axial load ratio was designed to induce a brittle flexural/shear failure. The test
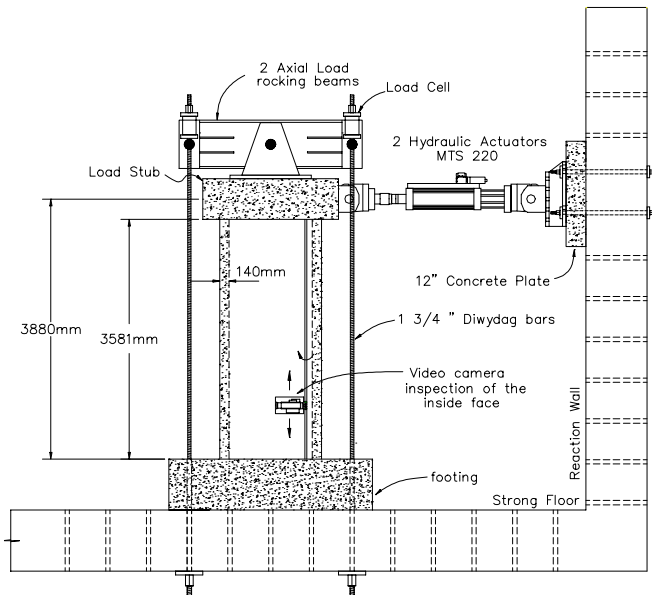
Figure 2 – Test setup
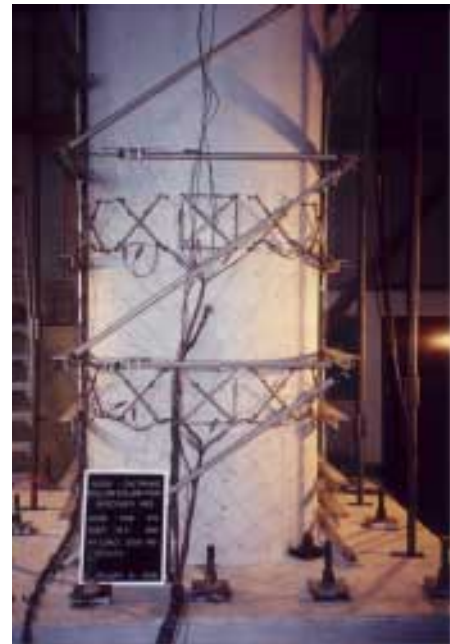
Figure 3 - Unit HS3 during testing

setup adopted for the three tests is shown in fig.2.

Units were tested with a cantilever scheme, under pseudo-static cyclic loading. The specimens were anchored to the strong floor via a shallow post-tensioned footing, with the aid of 18 prestressing bars. The lateral load was

applied on the column top with a couple of hydraulic actuators working in parallel. The axial load device consisted of two steel I beams, mounted on the column top stub via two rockers. Four prestressing bars were attached at the beam ends and anchored to the strong floor to apply the vertical force.

The inside of the column was monitored with the aid of a video camera. A device was built in order to rotate and move the camera up and down to guarantee the view of ¾ of the inside surface.

Lateral actions were applied alternatively in the push and pull directions, following a standard loading protocol. Elastic cycles were conducted in load control up to theoretical first yield of longitudinal rebars, while inelastic cycles were conducted for increasing levels of displacement ductility (μ=1.0,1.5,2.0,3.0,4.0,6.0), with 3 repeated cycles at each ductility level.

The instrumentation consisted of 160 strain gauges mounted in several locations along the main longitudinal bars and on the continuous spiral. In addition to the gauges, displacement transucers were used to measure the column flexural and shear displacement components. As visible from the photo of figure 3, 8 curvature cells were mounted along the column height. Two shear deformation panels were instead mounted on the column sides, each consisting of three main blocks. In addition to this instrumentation, two sets of small shear panels were mounted in two "strategic" sections, with the objective of measuring the local shear behavior within the region that is more critical
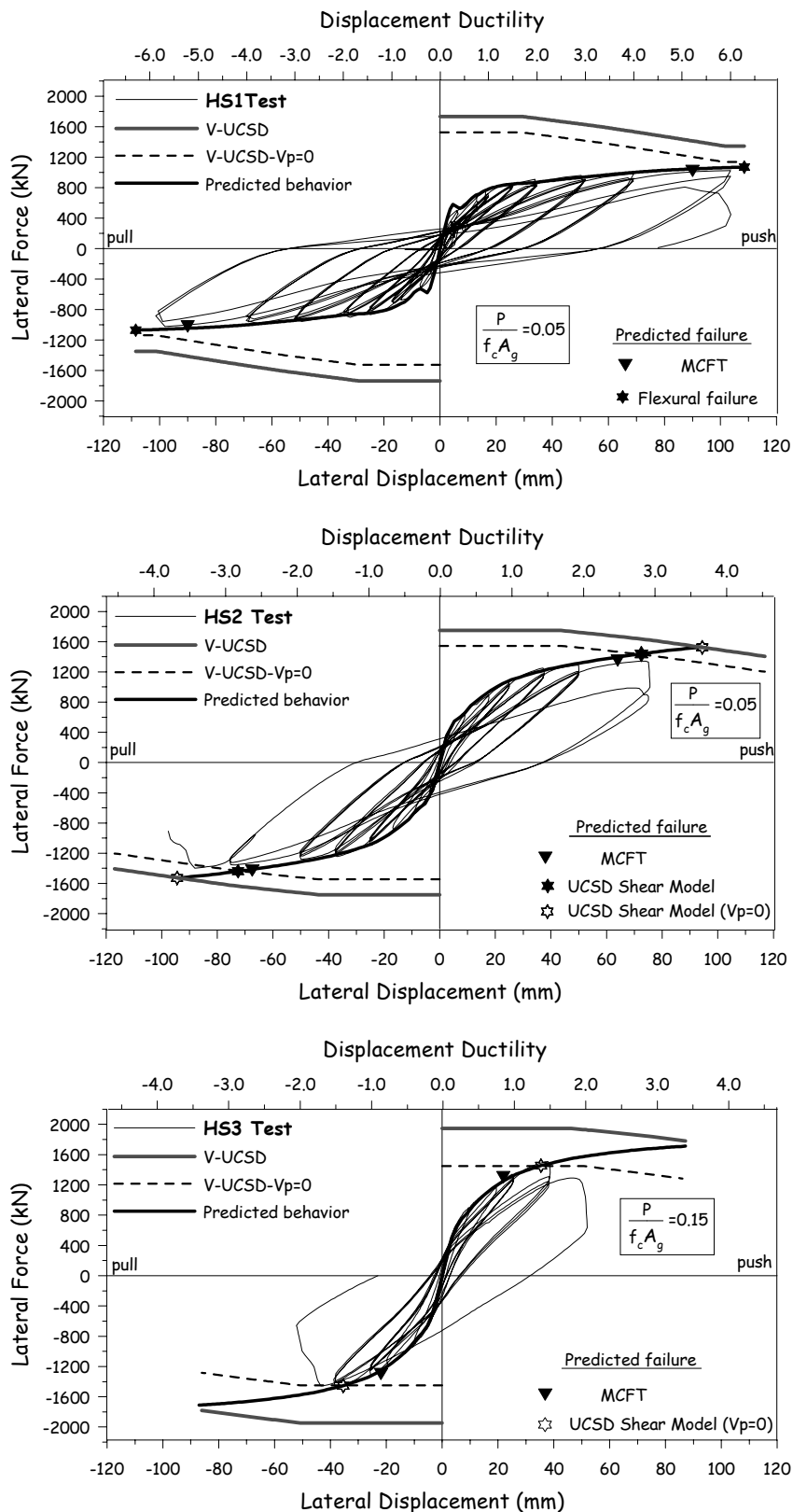
Figure 4 – Force-displacement response of units HS1, HS2 and HS3

for shear. For these square deformation panels (visible in figure 3), a size of 305mm, about 3 times the expected diagonal crack spacing, was selected in order to accurately measure the average behavior of a small portion of the specimen

EXPERIMENTAL RESULTS

with the predicted shear strength envelopes and with the predicted monotonic load-deformation behavior. The shear strength envelopes were calculated with the UCSD-A model, with and without the axial load component V_p (for simplicity the UCSD-A model will be denoted in the following as UCSD). The load deformation predicted curves refer to the sectional analysis procedure described above in section 2.
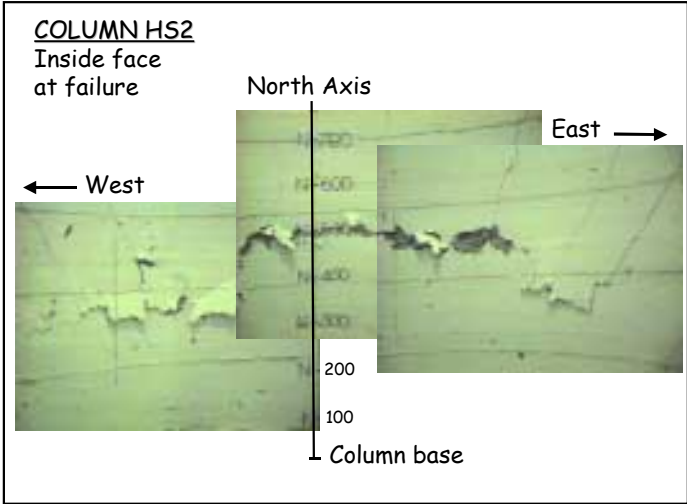
Figure 5 - Column HS2 – Inside face at failure

The load-deformation behavior predicted with the MCFT is not reported in the graphs, since it is very similar to that obtained with sectional analysis. In each graph, the predicted failure points according to the considered models are also indicated.

In the first unit a flexural failure was expected, since the shear strength envelope does not intersect the predicted load-deformation curve. Note that flexural failure is predicted both with the MCFT and with the UCSD model (with or without inclusion of the axial load effect). However, while the MCFT predicted a flexural failure due to concrete crushing in compression, the sectional analysis

with the UCSD model predicted flexural failure due to high strain in the longitudinal reinforcement in tension (>6%). Failure of the test unit was observed at ductility 6.0 due to implosion of concrete in the inside face of the column wall. Buckling of longitudinal rebars occurred in the compression region at column base, involving 4

layers of spiral reinforcement. Note that before failure at ductility 6.0, limited strength degradation occurred during repeated cycles. The test results confirmed that the predicted failure mode was correct. The load deformation predicted behavior matched well the experimental response. Note during the inelastic stages of testing, shear deformations accounted for 30% of the total displacement at the column top. The ultimate displacement capacity was slightly underestimated with the MCFT.

During the response of unit HS2, little strength degradation occurred before ductility 3.0, when concrete spalling in the inside face occurred (fig.5). This caused a sudden loss in strength of approximately 25%. The unit subsequently failed in shear at ductility 3.5 (see fig.6), with a large inclined crack forming in the column base region. The transverse steel fractured along the crack in several layers. Also in this case the predicted load-deformation curve matched very well the experimental response. The ultimate point happened to be between the two predicted with the UCSD model (with and without the axial load component). As for the previous unit, the MCFT underestimated slightly the deformation capacity. This model predicted shear failure at ductility 2.4 due to rupture of transverse steel.

The behavior of unit HS3 was greatly influenced by the higher level of axial load. The force-displacement cycles, showed a more evident pinched shape near the origin, due to the effect of

Figure 6 - Unit HS2 at failure

the axial load. Concrete spalling in the inside face occurred at ductility 2.0 in the push direction, and subsequently the unit failed in the first cycle in the pull direction. In this case the load deformation response was again well predicted and the ultimate point was appropriately estimated by the UCSD model without the V_p component. The ultimate point predicted by the MCFT significantly underestimated the deformation capacity in this case.

In Table 3, the experimental values of shear force and displacement at failure are compared with the ones predicted by the UCSD model (with the two options of including or neglecting the axial load effect) and by the MCFT. From this preliminary examination, it seems that all considered models predicted the ultimate strength and failure mode with reasonable accuracy. The deformation capacity instead is well predicted only by the UCSD model when the axial load component V_p is neglected. In general it appears that the estimates made with the MCFT of both deformation capacity and strength are a little conservative.

Table 3 – Predicted and experimental values of shear force and displacement at failure

Unit	V_{exp} (kN)	Δ_{exp} (mm)	V_{UCSD} (kN)	Δ_{UCSD} (mm)	V_{UCSD}-V_p (kN)	$\Delta_{UCSD}(V-V_p)$ (mm)	V_{MCFT} (kN)	Δ_{MCFT} (mm)	Failure mode*
HS1	972	103	1069	108	1069	108	1020	90	F
HS2	1396	88	1526	94	1438	73	1350	64	S
HS3	1457	52	1780	87	1454	35	1300	22	S

*F = flexure, S = shear
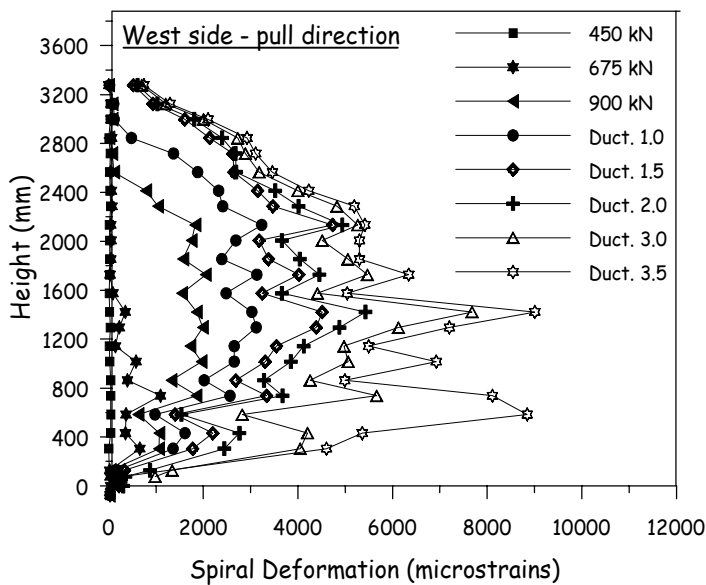
Figure 7 – Unit HS2 – Trans. strain profiles

A further understanding of the shear behavior can be obtained by analyzing the strains in the transverse reinforcement. Two aspects are particularly relevant in this matter : 1) the lateral strain distribution along the column height and 2) the behavior of lateral strains as a function of the applied lateral displacement.

If the lateral strains of unit HS2 at section mid-depth are considered, profiles can be plotted as a function of the column height for each level of applied load or displacement (see figure 7). It can be noted that before significant diagonal cracking occurs during the elastic cycles (up to the 450kN cycle), the deformation in the spiral reinforcement is exactly zero. Subsequently (in the 675kN cycle), deformations appear in the base region (within one column diameter above the base) and progressively move up further towards the column top, as the applied lateral load increases. Maximum values occur at approximately one column diameter above the base. It can be noted that large strains occur only between 0.5 and 1.5 section diameters above the base. This is the so called "shear-critical" region, where the interaction between shear and flexure produces more damage. In the first 500mm above the base lower strains occur due to the confining effect generated by the presence of the foundation footing.

In fig.8 the strains in the transverse reinforcement at section mid-depth are plotted as a function of the displacement at the column top. Experimental values

Figure 8 – Unit HS2 - transverse steel behavior

are plotted for three different locations (at 305, 876 and 1435mm above the column base). In the same graph, the predicted average behavior obtained with the UCSD model and with the MCFT are plotted. The predicted behavior according to the UCSD model is obtained with the procedure described in section 2. The behavior predicted with the MCFT agrees quite well with the response in the section at 1435mm above the base, while that obtained from the UCSD model is closer to that at 876mm above the base.

The strain activation is accurately predicted by the MCFT and by the UCSD without V_p at approximately 5mm lateral displacement (corresponding to a load of 600kN). The UCSD model without V_p predicts that the trasverse reinforcement will yield at a displacement of 75mm, while the MCFT predicts yielding at 35mm. Comparing these results with those from figure 7, it can be observed that yielding of transverse steel (3800 $\mu\varepsilon$) occurred at ductility 1.5 (40mm) thus indicating that the estimate made with the MCFT was more accurate.

CONCLUSIONS

are the thickness of the wall and the flexural capacity. For the same shear strength, members with higher flexural capacity require thicker walls to prevent concrete spalling in the inside surface.

The ultimate shear strength and deformation capacity can be predicted with reasonable accuracy by using recent shear strength equations. Some modifications are needed to properly account for the particular shape of the section and for the effect of the axial load. The same model can be used successfully to predict the load-deformation behavior with sectional analysis. Shear deformations can be computed based on the expected level of average deformation in the transverse steel. Weather or not a shear failure is likely to occur is strongly dependent on the level of strain that develops in the transverse reinforcement. Detailed analysis of transverse strains in the shear critical region may be used to accurately predict the failure mode.

From the results of this preliminary study, it is suggested the effect of axial load on shear strength be neglecte

REFERENCES

Modified Compression Field Theory" – *Users manual,* University of Toronto, Canada

Collins, M.P., Vecchio, F.J. (1988) "Predicting the Response of Reinforced Concrete Beams Subjected to Shear using Modified Compression Field Theory", *ACI Structural Journal,* May-June 1988

Paulay, T., Priestley, M.J.N. (1992) "Seismic Design of Reinforced Concrete and Masonry Structures", John Wiley and Sons, New York, 1992

Priestley, M.J.N., Kowalsky, M.J., Vu, N., Mc Daniel, C. (1998) "Comparison of Recent Shear Strength Provisions for Circular Bridge Columns" *Proceedings of the Fifth Caltrans Seismic Workshop,* Sacramento, July 1998.

Priestley, M.J.N., Ranzo, G., Kowalsky, M.J., Benzoni, G. (1996) "Yield Displacement of Circular Bridge Columns" *Proceeding of the Fourth Caltrans Seismic Workshop,* Sacramento, July1996.

Tokyu Construction Company, (1998) "Test Notes on Hollow Bridge Columns", Unpublished report, Tokyo, Japan.

Whittaker, D., Park, R., Carr, A.J., (1987) "Experimental Tests on hollow Circular Concrete Columns for Use in Offshore Concrete Platforms" , *Proceedings of the 3rd Pacifc Conference on Earthquake Engineering*, New Zealand, 1987.

Zahn, F.A., Park, R. and Priestley, M.J.N., (1990) " Flexural Strength and Ductility of Circular Hollow Reinforced Concrete column without Confinement on Inside Face", *ACI Structural Journal*, March-April 1990